UCRL-JC-132052
Preprint

Coupled THM Analysis of the Single-Heater Test at Yucca Mountain

S. C. Blair, W. Lin, A. L. Ramirez, W. D. Daily and T. A. Buscheck

This paper was prepared for submittal to
37th U.S. Rock Mechanics Symposium
Vail, CO
June 6-9, 1999

January 25, 1999

Lawrence Livermore National Laboratory

Coupled THM analysis of the Single-Heater Test at Yucca Mountain

S.C. Blair, W. Lin, A.L. Ramirez, W.D. Daily, T.A. Buscheck
Lawrence Livermore National Laboratory, USA

ABSTRACT: This paper presents a summary of results from the Single-Heater Test (SHT) at Yucca Mountain, Nevada. In the SHT, a horizontal, 5-m-long, line-heat source was used to heat a rock pillar for nine months. Moisture movement was monitored during and after heating using electrical-resistance tomography (ERT) and neutron-logging techniques. Results indicate drying in regions of the rock where temperature reached 60°C and above. The drying zone is asymmetric and is not centered on the heater, but has lobes extending above and to the sides of the heater. Predicted temperatures agreed well with observations. A cold-trap effect was predicted, in the heater borehole, that efficiently transfers heat along the heater borehole to the excavation wall. A simple thermomechanical analysis of the SHT shows that shear zones predicted for vertical fractures coincide with regions of increased moisture content derived from ERT measurements.

1 INTRODUCTION

The Single-Heater Test (SHT) was one phase of the field-scale thermal testing program of the Yucca Mountain Site Characterization Project (YMP). The purpose of the SHT was to study the coupled thermal–hydrologic–mechanical–chemical (THMC) behavior of the Topopah Spring tuff, and the test was conducted in an alcove excavated off of the Exploratory Studies Facility at Yucca Mountain, Nevada. The rock in this unit is a densely welded, nonlithophysal, ashflow tuff.

In this test a 5-m-long line-heat source was used to heat a rock pillar for approximately nine months. After the heater was turned off, the rock mass was monitored during the cool-down for another nine months, until May 28, 1997, when the test was terminated. Figure 1 shows the general layout of the SHT, including the boreholes that were drilled perpendicular to the heater to monitor moisture movement along the approximate midplane of the test.

The SHT was a cooperative effort conducted by the YMP thermal test team, which includes participants from four national laboratories (Lawrence Livermore National Laboratory, Lawrence Berkeley National Laboratory, Los Alamos National Laboratory, and Sandia National Laboratories), the U.S. Geological Survey, and the YMP Management and Operating contractor. The THMC response of the rock mass to heating was monitored by several different types of measurements, only a few of which are reported here. Thermal neutron logging and elec-

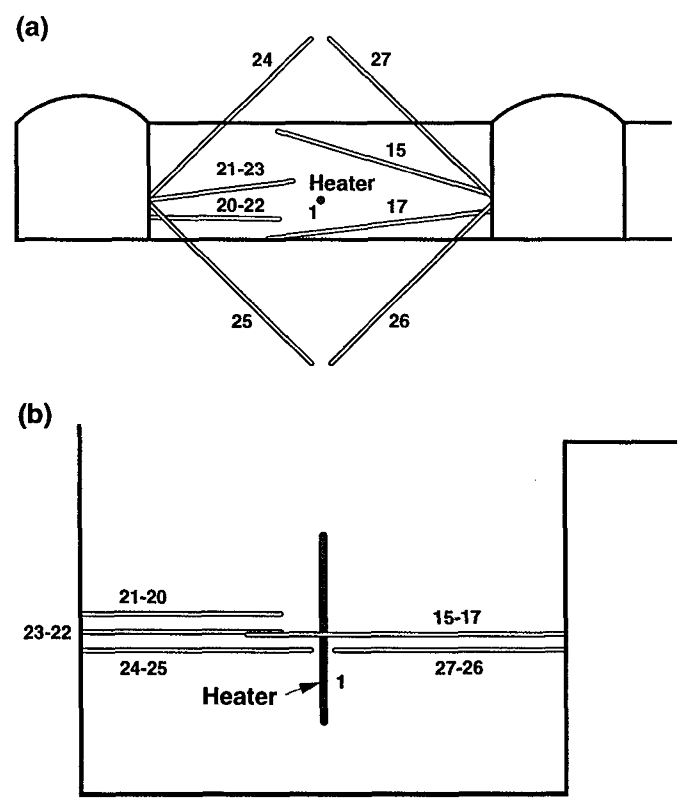

Figure 1. Layout of the Single-Heater Test
a) Vertical cross section of the test, showing excavations, theater borehole, and other selected boreholes
b) Plan view of the layout, showing excavations and selected boreholes (from Blair et al. 1998)

trical-resistance tomography (ERT) were among the techniques used to monitor the rock's water saturation over time with the intent of estimating the movement of steam condensate out of the system. Section 2 of this paper presents a brief discussion of these methods and results and of the temperature history of the test. Section 3 presents a summary of thermohydrologic (TH) and thermomechanical (TM) simulations conducted for the SHT.

2 TEMPERATURE AND MOISTURE MEASUREMENTS

One goal of the SHT was to raise rock temperature near the heater to approximately 140°C and then to monitor the predicted ensuing dry-out. Figure 2 shows the temperature history of a thermocouple located near the heater midplane and within 0.25 m (radially) of the heater. This figure shows that temperature in the rock near the heater rose rapidly after the heater was turned on, reaching 100°C at approximately 25 days after the start of heating. Temperature then increased smoothly with heating, reaching 140°C after 270 days of heating, when the heater was turned off. Temperature in the rock near the heater dropped quickly after the heater was turned off, cooling to approximately 50°C after 30 days of cooling (300 days from start of heating). A few power outages occurred during the heating phase of this test, causing the temperature to drop rapidly during the outage, and then recover to near pre-outage levels when power was restored. These outages are evidenced by sharp drop/recovery episodes in the data.

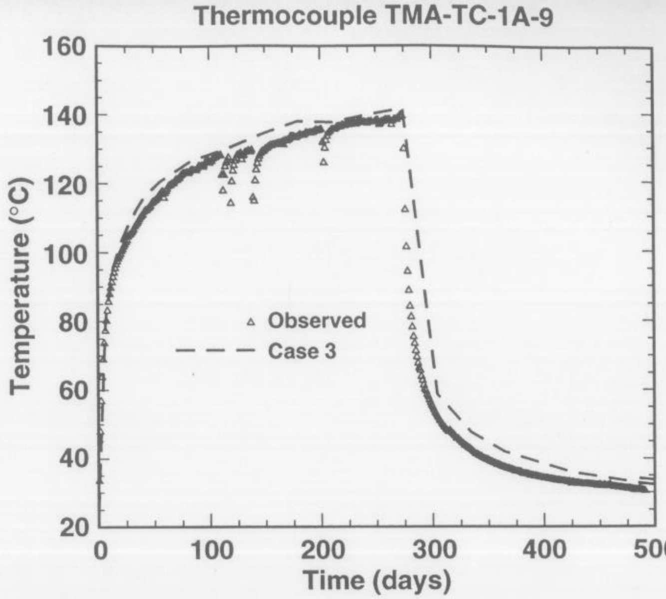

Figure 2. Temperature history of the SHT measured near the heater. Sharp drop/recovery episodes are due to power outages. Also shown are simulated temperatures calculated using the NUFT TH model. (from Blair et al. 1998)

Thermal neutron logging was used to monitor moisture content in four boreholes during the SHT. These are boreholes 15, 17, 22, and 23 in Figure 1. They are oriented perpendicular to the heater and in approximately the same plane as the ERT measurement holes. The neutron-logging tool provides an estimate of the amount of water in a region within about a 12-cm radius of the center of a borehole.

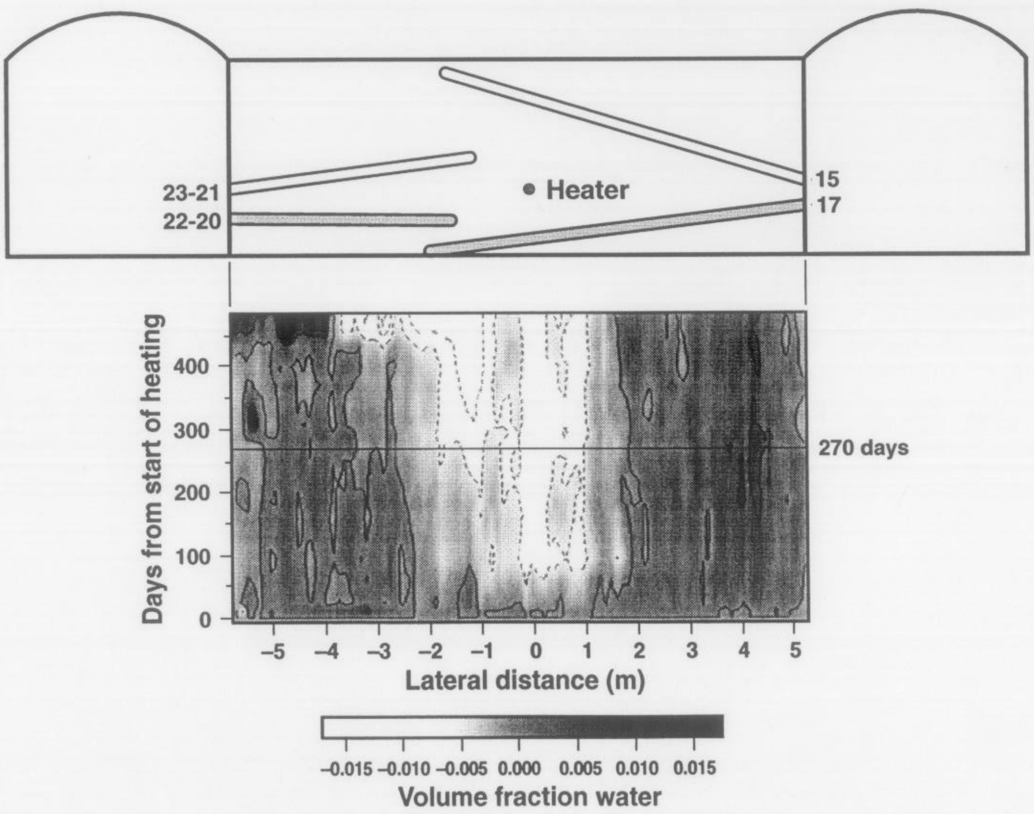

Figure 3. Moisture movement during the SHT, along a line perpendicular to and slightly below the heater, as derived from neutron logging measurements

Logs were taken prior to the start of heating and then approximately once a month throughout the SHT. Logs showing change in moisture along a given hole were produced by comparing logs collected on a given day with logs collected prior to the start of heating. A series of these moisture-change logs for boreholes 17 and 22 were used to compute an image (Figure 3) of moisture change over time for a line passing approximately 1 m under and perpendicular to the heater. Figure 3 shows that a dry zone approximately 4 m wide develops within the first 100 days of heating. This zone is asymmetric about the heater with the drying region extending farther from the heater on its left (negative distance) side. Moreover, drying immediately below the heater started as early as 25 days after the start of heating. This figure also shows that the width of the drying zone continued to increase even after the end of heating at 270 days, and no rewetting is evident in zones that were dried by the heating. This figure also indicates that, during the cool-down period, an increase in moisture occurs near the northern (left) drift. It is also important to note that temperature measurements in the neutron holes indicated that drying occurred at temperatures in the range of 60° to 90°C.

ERT was also used to monitor moisture movement in this test. ERT is a geophysical imaging technique that can be used provide tomographs of subsurface resistivity. Moreover, if the spatial distribution of temperature in the plane of the tomograph is known, then an inversion technique can be used to estimate the spatial distribution of saturation change in the plane of the measurement.

The ERT measurements were are made with an automated data-collection system and consist of voltage and current measurements from a series of electrodes. The electrodes were emplaced in boreholes 24–27, shown in Figure 1, to image resistivity in a cross section perpendicular to the heater and midway along the heater length. The data are then processed to produce electrical-resistance tomographs that show changes in electrical resistivity as a function of space and time. To calculate changes in the rock's electrical resistivity, a data set obtained after heating started was compared to a corresponding data set obtained prior to heating, and tomographs of these data were constructed. Saturation estimates were then calculated using a version of the Waxman–Smits equation (Waxman & Thomas 1974a, b) that assumes dominant surface conductance, the resistivity-ratio tomographs, and maps of interpolated temperatures.

Results of ERT at the end of the heating phase (270 days of heating) are shown in Figure 4, along with the temperature field computed for that time. This figure shows that heating of the rock generally caused drying (decreased liquid saturation) near and above the heater and wetting (increased liquid saturation) in rock below and to the north of the heater. The most extensive drying is observed in regions at the heater elevation and above. However, the dry zone detected by ERT is not centered on the heater and is not symmetric about the heater; rather, it has lobes that extend upward from and to either side of the heater. The ERT measurements do indicate that

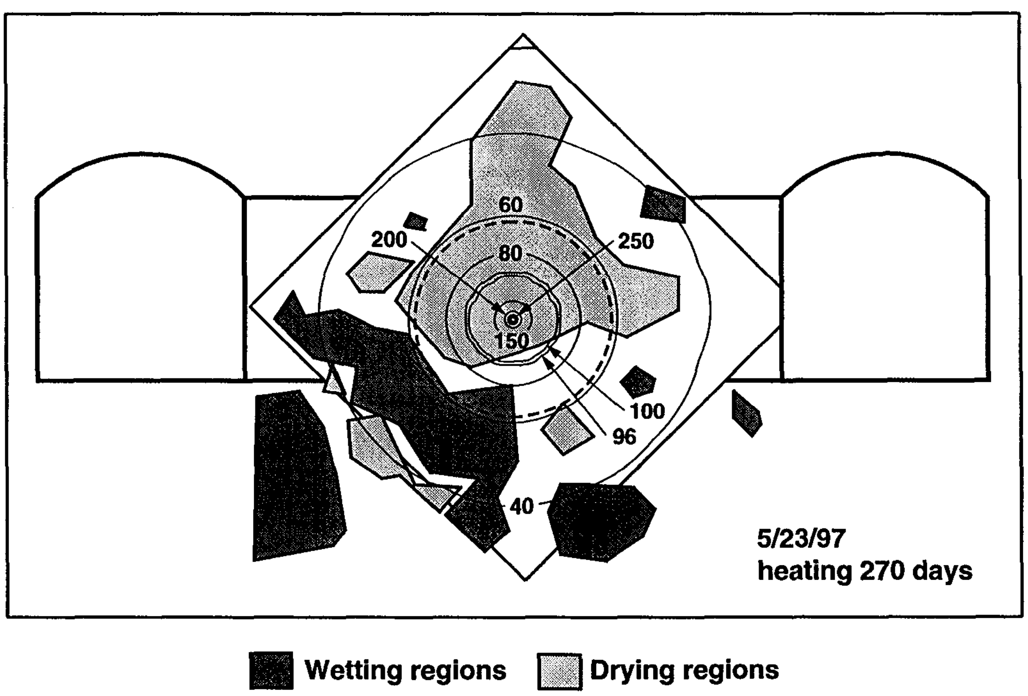

Figure 4. Zones of drying and wetting, derived using ERT. Contour lines are predicted temperatures (°C) computed using the DKM model.

the driest region was right around the heater and that it had a saturation of approximately 10%. This figure also shows that, for the region below the heater, measurable drying is indicated for rock at temperatures greater than 60°C.

Comparison of the neutron-logging and ERT data collected throughout the test show the two data sets to be in good agreement (Blair et al. 1998).

The saturation estimates suggest that, during the heating phase, a region of drying formed around the heater. This may be because, as the temperature increases above ambient, the vapor pressure in the pores increases. Fractures connected pneumatically to the drift provide a pressure gradient so that moisture leaves the rock through fracture openings and moves along the fractures in response to buoyancy or thermally driven pressure gradients.

The estimates also suggest that rock on either side of the heater and a couple of meters below its elevation showed the highest saturation increases. We postulate that these wetter zones formed along fractures further away, where temperature and pressure conditions allowed condensation below the local dew point. This is consistent with results of a similar test conducted at the G-tunnel (Ramirez et al. 1991).

During the cooling phase, the dry region remained relatively stable. Wetter rock regions, which developed below the heater during the heating phase, became relatively smaller during the cooling phase, particularly below and to the north of the heater.

3 SIMULATIONS OF THE SHT.

TH behavior during the heating and cooling stages of the SHT was modeled with the NUFT code (Nitao 1998a, b). A primary purpose of the TH-model calculations was to compare simulated temperatures with the temperatures measured in the field during the heat-up and cool-down periods of the SHT. Comparison between simulated and measured temperatures is a useful way of assessing the applicability of the property set used in the calculation to predict TH behavior in one of the three major host-rock units. In addition, the model was used to assess the effect on the SHT of percolation flux through the formation.

The dual-permeability (DKM) conceptual model for fracture–matrix interaction was used in these simulations. This model accounts for disequilibrium processes between the fracture and matrix continua and includes the influence of vapor and heat flow along the heater borehole. Predicted temperatures, shown in Figure 2, are in excellent agreement with the observed temperatures throughout the heating stage of the SHT. The model also predicted a pronounced cold-trap effect in the heater borehole. Vapor and latent heat flowed from the heated interval of the heater borehole to the cool end of the heater borehole adjacent to its collar, where the vapor condensed, resulting in focused condensate drainage and a local increase in matrix saturation. The cold-trap effect efficiently transferred heat along the heater borehole toward the TM alcove. The cold-trap effect is a potentially important mechanism influencing TH behavior in emplacement drifts.

Knowledge of the percolation flux within the host formation is important for predicting long-term performance of a proposed repository. To assess the effect of percolation flux on the SHT, the test was simulated assuming flux values of 11.52 mm/yr and 0.22 mm/yr. Results show a negligible difference in simulated temperature for these two cases. This indicates that TH behavior in the SHT is insensitive to the magnitude of percolation flux. The SHT was not sensitive to this parameter because the heat-driven condensate fluxes were much greater than any of the values of percolation flux that were considered. Therefore, the SHT was not a useful test for diagnosing the magnitude of percolation flux. In general, any in situ thermal test that is relevant to TH behavior in a potential repository will generate heat-driven condensate fluxes during the heating phase that are much greater than ambient percolation flux. However, during the cool-down phase, the condensate fluxes will quickly decline to less than the ambient flux. If, in such a test, percolation is found to be the rate-limiting process controlling rewetting of the dry-out zone, that test may be useful for diagnosing the magnitude of the local percolation flux.

A simple TM analysis of the SHT was also conducted. This analysis was designed to assess the potential for TM stresses developed in the SHT to cause shear-slip on fracture sets occurring in the heated rock mass. Shear-slip has been shown to increase rock-mass permeability (Barton et al. 1997). Geologic mapping of the SHT and nearby excavations show that there are three fracture sets present in the rock mass (Albin et al. 1997): two vertical fracture sets (oriented N–S and E–W) and one sub-horizontal fracture set. For this study we estimated regions where slip may occur on the vertical fractures oriented in the E–W direction.

Figure 5 shows contours of the ratio of shear stress to shear strength on vertical E–W oriented fractures after 60 days of heating. Shear-slip on fractures can be expected in regions where the ratio is greater than 1.0 (these regions have been shaded for purposes of discussion). Figure 5 shows that zones of potential shear-slip develop relatively early in the heating phase of the test when thermal gradients and associated stress gradients are the largest. These zones are more or less symmetric about a vertical plane through the heater. In the area between the drifts and above the drift plane, shear-slip on vertical fractures can be expected in two large lobes, approximately 3 m in height, that arch from the drift walls, extending about 4 m toward the heater.

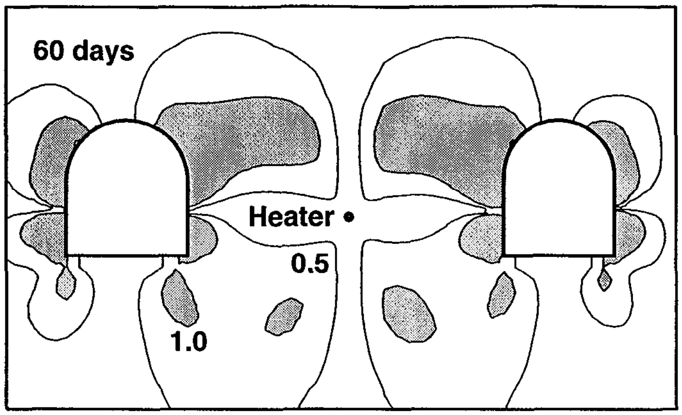

Figure 5. Ratio of shear stress to shear strength on fractures for 60 days of heating for the SHT. Ratios > 1.0 (shaded areas) indicate regions of predicted shear-slip.

Below the heater plane and between the drifts, zones of potential shear-slip 1–2 m in diameter are predicted along and below the drift wall. Zones approximately 2 m in diameter are also predicted 3–4 m below the heater and 1–2 m to either side of a vertical plane extending through the heater

As mentioned above, slip on fractures can change their hydraulic properties, and in Figure 6 zones of predicted shear-slip after 60 days have been overlaid with wetting zones observed using ERT at 59 days of heating. This figure shows that that some zones of predicted shear correlate directly with zones where increased rock saturation was observed.

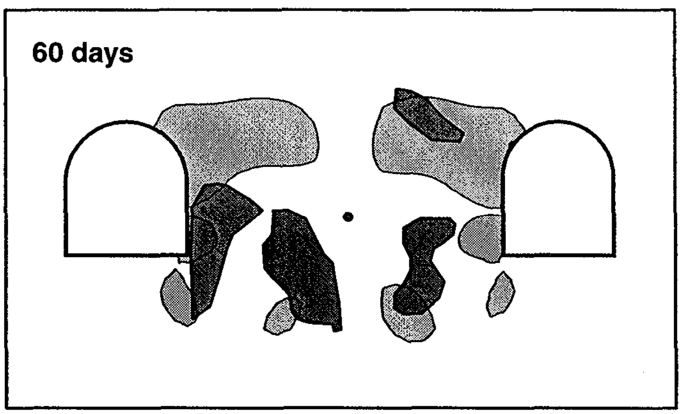

Figure 6. Regions of predicted shear-slip on vertical fractures for 60 days of heating (light shading), overlaid with zones of wetting observed for 59 days of heating (dark)

This correlation may indicate thermal–hydrologic–mechanical (THM) coupling in these areas. However, mechanisms of THM coupling are poorly understood. It is possible that shear-slip and associated dilation of fractures increased the porosity and permeability of the fractures and that this provided a new path for drainage or storage of some of the water shedding from above the heater. Another mechanism is that creation of new mineral surface area by shearing of the rock affected the water chemistry. Most minerals on fracture surfaces are high in calcium and magnesium; dissolution of these ions could increase the water conductivity.

4 CONCLUSIONS

Moisture movement in the SHT was monitored using neutron and ERT techniques. Results show drying in regions at the heater elevation and above. However, the dry zone is not centered on the heater and is not symmetric about the heater; rather, it has lobes that extend upward from and to either side of the heater (Figure 2). The ERT measurements do indicate that the driest region was right around the heater and that it had a saturation of approximately 10%. Both neutron and ERT techniques indicate that drying occurs in rock that is heated to temperatures of 60°C and above. It is interesting to note that this is the temperature where continuity of water films on tuff is lost.

TH modeling produced good agreement with observed temperatures and showed a pronounced cold-trap effect. TM modeling show some correlation between areas of predicted shear-slip on vertical fractures and regions of wetting.

REFERENCES

Albin, A.L., W.L. Singleton, T.C. Moyer, A.C. Lee, R.C. Lung, G.L.W. Eatman & D.L. Barr 1997. *Geology of the Main Drift—Station 28+00 to 55+00, Exploratory Studies Facility. Yucca Mountain Project, Yucca Mountain, Nevada.* Denver: Bureau of Reclamation and U.S. Geological Survey.

Barton, C.A., S. Hickman, R. Morin, M.D. Zoback, T. Finkbeiner, J. Sass & D. Benoit 1997. Fracture permeability and its relationship to in-situ stress in the Dixie Valley, Nevada, geothermal reservoir. In proceedings from *Twenty-Second Workshop on Geothermal Reservoir Engineering.* January 27–29, 1997. Stanford, CA: Stanford University.

Blair, S.C., T.A. Buscheck, L.D. DeLoach, W. Lin & A.L. Ramirez 1998. *Single-Heater Test final report.* (UCRL-ID-131491) Livermore, CA: Lawrence Livermore National Laboratory.

Nitao, J.J. 1998a. *Reference manual for the NUFT flow and transport code, version 2.0.* (UCRL-MA-130651) Livermore, CA: Lawrence Livermore National Laboratory.

Nitao, J.J. 1998b. *User's manual for the USNT module of the NUFT code, version 2.0 (NP-phase, NC-component, thermal).* (UCRL-MA-130653) Livermore, CA: Lawrence Livermore National Laboratory.

Ramirez, A.L., R.C. Carlson & T.A. Buscheck 1991. *In situ changes in the moisture content of heated, welded tuff based on thermal neutron measurements.* (UCRL-ID-104715) Livermore, CA: Lawrence Livermore National Laboratory.

Waxman, M.H. & E.C. Thomas 1974a. Electrical conductivities in shaly sands: I. The relation between hydrocarbon saturation and resistivity index. *J. Petrol. Tech.* Feb:213–218 (Transactions AIME, 257).

Waxman, M.H. & E.C. Thomas 1974b. Electrical conductivities in shaly sands: II. The temperature coefficient of electrical conductivity. *J. Petrol. Tech.* Feb:218–225 (Transactions AIME, 257).

Work performed under the auspices of the U.S. Department of Energy by the Lawrence Livermore National Laboratory under Contract W-7405-Eng-48.